Fermi Surface, Surface States, and Surface Reconstruction in Sr_2RuO_4

A. Damascelli, D. H. Lu, K. M. Shen, N. P. Armitage, F. Ronning, D. L. Feng, C. Kim, and Z.-X. Shen
Department of Physics, Applied Physics and Stanford Synchrotron Radiation Laboratory, Stanford University, Stanford, California 94305

T. Kimura and Y. Tokura
Department of Applied Physics, The University of Tokyo, Tokyo 113-8656, Japan and JRCAT, Tsukuba, 305-0046, Japan

Z. Q. Mao and Y. Maeno
Department of Physics, Kyoto University, Kyoto 606-8502, Japan and CREST-JST, Kawagushi, Saitama 332-0012, Japan
(Received 2 May 2000)

The electronic structure of Sr_2RuO_4 is investigated by high angular resolution ARPES at several incident photon energies. We address the controversial issues of the Fermi surface (FS) topology and the van Hove singularity at the M point, showing that a surface state and the replica of the primary FS due to $\sqrt{2} \times \sqrt{2}$ surface reconstruction are responsible for previous conflicting interpretations. The FS thus determined by ARPES is consistent with the de Haas–van Alphen results, and it provides additional information on the detailed shape of the α, β, and γ sheets.

PACS numbers: 74.25.Jb, 74.70.Ad, 79.60.Bm

Angle-resolved photoemission spectroscopy (ARPES) has proven itself to be an extremely powerful tool in studying the electronic structure of correlated electron systems. In particular, in the case of the high-temperature superconductors, it has been very successful in measuring the superconducting gap, determining the symmetry of the order parameter, and characterizing the pseudogap regime [1]. On the other hand, one of the fundamental issues, namely, the determination of the Fermi surface (FS) topology, has been controversial, as in the case of $Bi_2Sr_2CaCu_2O_8$, raising doubts concerning the reliability of the ARPES results. A similar controversy has also plagued the fermiology of Sr_2RuO_4. In this context, the latter system is particularly interesting because it can also be investigated with de Haas–van Alphen (dHvA) experiments, contrary to the cuprates, thus providing a direct test for the general reliability of the photoemission results.

Whereas dHvA analysis, in agreement with local density approximation (LDA) band-structure calculations [2,3], indicates two electronlike FS (β and γ) centered at the Γ point, and a hole pocket (α) at the X point [4–6], early ARPES measurements suggested a different picture: one electronlike FS (β) at the Γ point and two hole pockets (γ and α) at the X point [7,8]. The difference comes from the detection by ARPES of an intense, weakly dispersive feature at the M point just below E_F that was interpreted as an extended van Hove singularity (evHS) pushed down below E_F by electron-electron correlations [7,8]. With the evHS below E_F, rather than above (LDA band-structure calculations place it 60 meV above E_F [2,3]), the γ pocket is converted from electronlike to holelike. The existence of the evHS was questioned in a later photoemission paper [9], where it was suggested that dHvA and ARPES results could be reconciled by assuming that the feature detected by ARPES at the M point was due to a surface state (SS). Recently, two possible explanations were proposed. First, the evHS at the M point could be only slightly above E_F (e.g., 10 meV), so that considerable spectral weight would be detected just below E_F [10]. Alternatively, ARPES could be probing ferromagnetic (FM) correlations reflected by the existence of two different γ-FS (holelike and electronlike, respectively, for majority and minority spin directions), which might have escaped detection in dHvA experiments [11]. Second, the surface reconstruction as detected by low-energy electron diffraction (LEED), which has been proposed to be indicative of a FM surface [12], would also complicate the ARPES data. The resolution of this controversy is important not only for the physics of Sr_2RuO_4 *per se* but also as a reliability test for FS's determined by ARPES, especially on those correlated systems where photoemission spectroscopy is the only available probe.

In this Letter, we present a detailed investigation of the electronic structure of Sr_2RuO_4. By varying the incident photon energy and the temperature at which the samples were cleaved, we confirm the SS nature of the near-E_F peak detected at the M point, and we identify an additional dispersive feature related to the "missing" electronlike FS (γ). A complete understanding of the data can be achieved only by recognizing the presence of shadow bands (SB), due to the $\sqrt{2} \times \sqrt{2}$ surface reconstruction which takes place on cleaved Sr_2RuO_4 (as confirmed by LEED). Despite the surface complications, the FS as determined by ARPES is consistent with the dHvA results [4–6], and provides additional information on the detailed shape of the α, β, and γ sheets.

 0031-9007/00/85(24)/5194(4)$15.00

ARPES data were taken at the Stanford Synchrotron Radiation Laboratory (SSRL) on the normal incidence monochromator beam line equipped with a SES-200 electron analyzer in angle-resolved mode. With this configuration it is possible to simultaneously measure multiple energy distribution curves (EDC's) in an angular window of $\sim 12°$, obtaining energy-momentum information not at one single k point but along an extended cut in k space. The angular resolution was $0.5° \times 0.3°$ [$0.3°$ along the cut, corresponding to a k resolution of 1.5% of the Brillouin zone (BZ), with 28 eV photons]. The energy resolution was 14 meV, for high-symmetry cuts and photon energy dependence, and 21 meV, for the FS mappings. Sr_2RuO_4 single crystals were oriented by Laue diffraction and then cleaved *in situ* with a base pressure better than 5×10^{-11} torr. In order to compensate for the angular response of the analyzer, EDC's in a single cut were normalized against those measured on polycrystalline gold. Different cuts were then normalized with respect to each other on the basis of the spectral weight above E_F integrated in both momentum and energy.

In order to begin the discussion of our experimental results, let us first give an overview of the very rich photoemission spectra, introducing all of the features we will focus on throughout the paper. Figure 1 presents EDC's along the high-symmetry directions for Sr_2RuO_4 cleaved and measured at 10 K. The α, β, and γ sheets of FS expected on the basis of LDA calculations [2,3] and dHvA experiments [4–6] are indicated, together with the experimentally measured cuts, in the sketch depicting one-fourth of the 2D projected zone (PZ). All of the features in the data are labeled by following the assignments which will be given in the course of the paper. Along Γ-M, two peaks emerge from the background, disperse towards E_F, and cross it before the M point, defining β and γ electronlike pockets (Fig. 1a). Along M-X, a peak approaches and crosses E_F before the X point, defining, in this case, the α hole pocket centered at X (Fig. 1b). Similar results were obtained along Γ-X (Fig. 1c): the β pocket is clearly resolved, while α and γ crossings are almost coincidental. In addition, we identify a weak feature which shows a dispersion opposite to the primary peaks along Γ-M and Γ-X (SB, see below). Around the M point a sharp peak is observed (SS), whose weak dispersion along M-X can be followed until it crosses E_F and loses intensity. The highest binding energy along the dispersion (which is symmetric with respect to Γ-M) is found at the M point. Because of this behavior, the SS peak was initially associated with a sheet of FS centered at the X point and considered to be holelike in character [7,8].

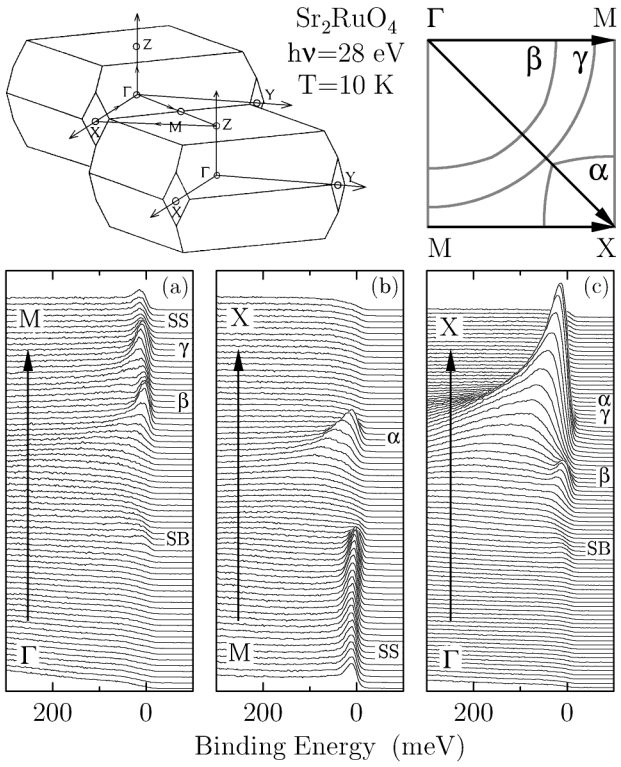

FIG. 1. ARPES spectra from Sr_2RuO_4 along the high-symmetry lines Γ-M, M-X, and Γ-X. As shown in the sketch of the 3D BZ, M is the midpoint along Γ-Z and, together with Γ and X, defines the 2D PZ. In the quadrant of the 2D PZ, the α, β, and γ sheets of FS are indicated together with the experimentally measured cuts.

In the following discussion, we will concentrate on the features observed near the M point, which are relevant to the controversy concerning the character of the γ sheet of FS. We will show that by working at 28 eV photon energy with sufficient momentum resolution both the β and γ electronlike pockets (predicted by LDA calculations [2,3]) are clearly resolved in the ARPES spectra. In order to address this issue, we measured the M point region (with cuts along Γ-M-Γ), varying the incident photon energy between 16 and 29 eV, in steps of 1 eV. Here, we covered the location of β and γ pockets in both first and second zones for better illustration (i.e., four E_F crossings will be observed). From the EDC's shown in Fig. 2 for 16, 22, and 28 eV, we can see that the cross sections of SS, β, and, *in particular,* γ exhibit a strong (and different) dependence on photon energy (note that by working at lower photon energies the momentum resolution increases and, in turn, the number of EDC's becomes progressively larger when going from panel c to panel a). At 28 eV, β and γ crossings can be individually identified in the EDC's. Owing to the high momentum resolution, we can now follow the dispersion of the γ peaks until the leading edge midpoints are located beyond E_F. After that, the peaks lose weight and disappear, defining the k_F vectors for the electronlike γ pockets. Right at k_F we can resolve a double structure which then reduces to the nondispersive feature (SS) located 11 meV below E_F. The difference between the 28 eV results and those obtained at 16 or 22 eV is striking (the latter are consistent with those previously reported at similar photon energies [7,8]). At low photon energies, the β crossings are still clearly visible. On the other hand, we can follow only the initial dispersion of the γ peaks (now broad and weak), before they merge with the SS feature,

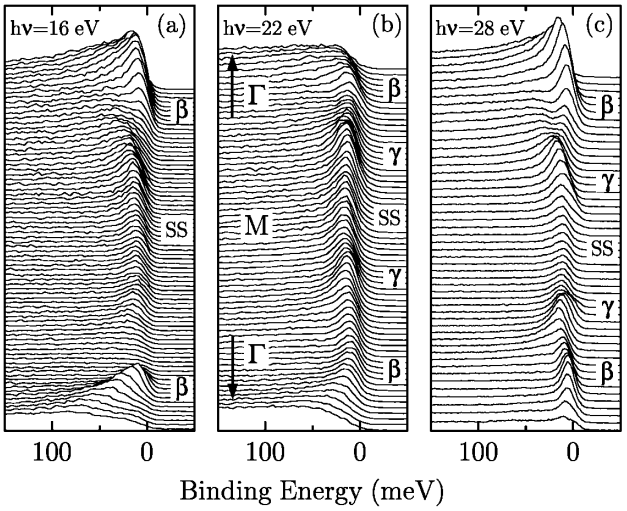

FIG. 2. ARPES spectra along Γ-M-Γ, at three different photon energies. The cuts are centered at the M point and extend beyond the γ and β FS crossings in both the first and second zones.

giving the impression of an evHS. At 16 eV it is impossible to identify the γ crossings. At 22 eV the location of the leading edge midpoints is at best suggestive of the presence of the γ crossings.

We have shown that the γ electron pocket had so far escaped detection in ARPES because it is indistinguishable from the SS feature at low photon energy and/or low angular resolution. In order to have a full picture of the relevant issues to be addressed, let us proceed to the discussion of the FS mapping. Figure 3b shows the E_F intensity map obtained at 28 eV on a Sr_2RuO_4 single crystal cleaved and measured at 10 K. The actual EDC's were taken over more than a full quadrant of the PZ with a resolution of 0.3° (1°) in the horizontal (vertical) direction. The EDC's were then integrated over an energy window of ±10 meV about the chemical potential. The resulting map of 73 × 22 points was then symmetrized with respect to the diagonal Γ-X (to compensate for the different resolutions along horizontal and vertical directions). The α, β, and γ sheets of FS are clearly resolved, and are marked by red lines in Fig. 3b. In addition, Fig. 3b shows some unexpected features: besides the diffuse intensity around the M point due to the presence of the SS band, there are weak but yet well defined profiles (marked in yellow). They can be recognized as a replica of the primary FS, and are related to the weak SB features detected in the EDC's along the high-symmetry lines (Figs. 1a and 1c). This result is reminiscent of the situation found in $Bi_2Sr_2CaCu_2O_8$, where similar shadow bands are possibly related to antiferromagnetic correlations, or to the presence of two formula units per unit cell [1]. On the other hand, in Sr_2RuO_4 the origin of the SB is different: inspection with LEED reveals superlattice reflections corresponding to a $\sqrt{2} \times \sqrt{2}$ surface reconstruction (see Fig. 3a), which is responsible for the folding of the primary electronic structure with respect to the $(\pi, 0)$-$(0, \pi)$ direction. This reconstruction, which was found on all of the Sr_2RuO_4 samples, is absent in the cuprates. Quantitative LEED analysis of the surface shows a 9° rotation of the RuO_6 octahedra around the surface normal [12]. This leads to the 45° rotation of the in-plane unit cell and to the enlargement of its dimensions by $\sqrt{2} \times \sqrt{2}$ over that of the bulk. The reconstruction, which reveals an intrinsic instability of the cleaved surface, should be taken into account as the origin of possible artifacts in all surface sensitive measurements.

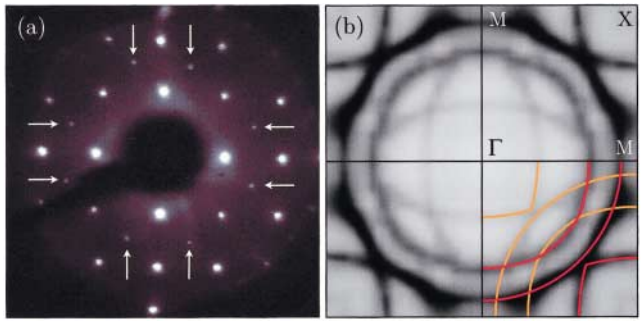

FIG. 3 (color). Panel (a): LEED pattern measured at 10 K with 450 eV electrons. The arrows indicate superlattice reflections due to $\sqrt{2} \times \sqrt{2}$ surface reconstruction. Panel (b): E_F intensity map. Primary α, β, and γ sheets of FS are marked by red lines, and replica due to surface reconstruction is marked by yellow lines. All data were taken on Sr_2RuO_4 cleaved at 10 K.

By inspecting the M point (Fig. 3b), it now becomes clear why the investigation of this k-space region with ARPES has been so controversial: in addition to the weakly dispersive SS feature (Figs. 1 and 2), there are several sheets of FS (primary and "folded"). At this point, the obvious question is, what is the nature of the SS feature? It has been proposed that it could be a surface state [9], and, in order to verify this hypothesis, we investigated its sensitivity to surface degradation by cycling the temperature between 10 and 200 K. We observed that the SS peak is suppressed much faster than all other features. Furthermore, by cleaving the crystals at 180 K and immediately cooling to 10 K we suppressed the SS, affecting the intensity of the other electronic states only weakly. A more sizable effect is observed on the SB, confirming a certain degree of surface degradation. However, this degradation was not too severe, as demonstrated by the LEED pattern taken after the measurements which still clearly shows the surface reconstruction (Fig. 4d). M-region EDC's, measured at 10 K (on a sample cleaved at 180 K), and corresponding intensity plots $I(\mathbf{k}, \omega)$ are shown in Figs. 4a and 4b. No signature of the SS is detected, and the identification of the Fermi vectors of α, β, and γ pockets is now straightforward. Performing a complete mapping on a sample cleaved at 180 K, we obtained an extremely well-defined FS (Fig. 4c). With the surface slightly degraded, we expect to see less of the relative intensity coming from SB and SS (note that the intensity scales in Figs. 3b and 4c, although not displayed, are identical). At the same time, we might also expect the primary FS to be less well defined, which is precisely *opposite* to what is observed. The FS shown in Fig. 4c

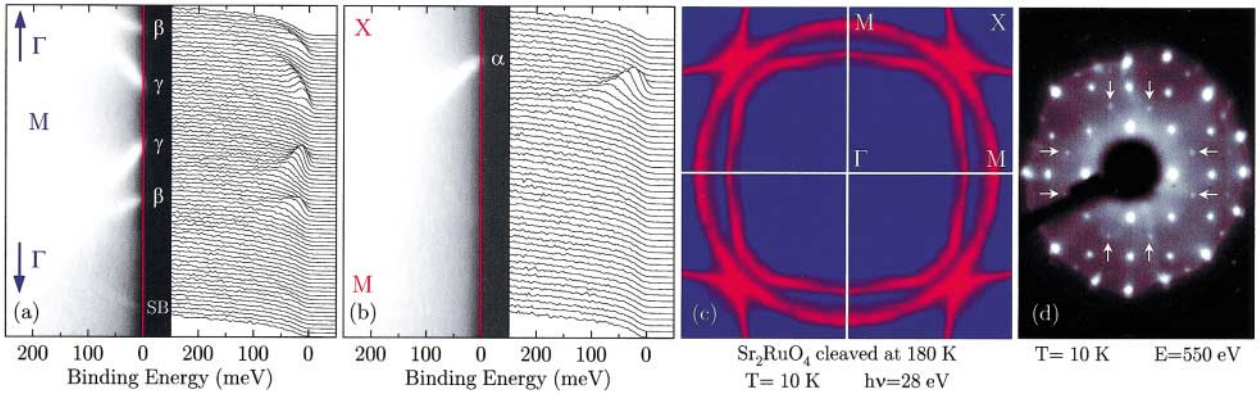

FIG. 4 (color). EDC's and intensity plot $I(\mathbf{k}, \omega)$ along Γ-M-Γ and M-X [panels (a) and (b), respectively]. Panel (c): E_F intensity map. Panel (d): LEED pattern recorded at the end of the FS mapping. All data were taken at 10 K on Sr_2RuO_4 cleaved at 180 K.

is in very good agreement with LDA calculations [2,3] and dHvA experiments [4–6]. The number of electrons contained in the FS adds up to a total of 4, in accordance with the Luttinger theorem, within an accuracy of 1% (as a matter of fact, for the FS determined on samples cleaved at 10 K the accuracy in the electron counting reduces to 3% due to the additional intensity of folded bands and surface state). As a last remark, we can confirm that α and β FS present the nested topology which has been suggested [13] as the origin of the incommensurate magnetic spin fluctuations later observed [14] in inelastic neutron scattering experiments at the incommensurate wave vectors $\mathbf{Q} \approx (\pm 2\pi/3a, \pm 2\pi/3a, 0)$.

Our results confirm the surface state nature of the SS peak detected at the M point. The comparison of Figs. 3b and 4c suggests that a surface contribution to the total intensity is also responsible for the less well-defined FS observed on samples cleaved at 10 K. At this point, one might speculate that these findings are a signature of the surface ferromagnetism recently proposed for Sr_2RuO_4 [11,12]. In this case, two different FS's should be expected for the two spin directions [11], resulting in (i) additional E_F weight near M due to the presence of a *holelike* γ pocket for the majority spin, and (ii) overall momentum broadening of the FS contours because the α, β, and γ sheets for the two spin populations are slightly displaced from each other in the rest of the BZ. Moreover, due to the surface-related nature of this effect, it would have escaped detection in dHvA experiments. In this scenario, a slight degradation of the surface would significantly suppress the signal related to FM correlations, due to the introduced disorder. The resulting FS would be representative of the nonmagnetic electronic structure of the bulk (Fig. 4c). The hypothesis of a FM surface seems plausible because the instability of a nonmagnetic surface against FM order is not only indicated by *ab initio* calculations [11] but it may also be related to the lattice instability evidenced by the surface reconstruction [12]. To further test this hypothesis, we suggest spin-polarized photoemission measurements and both linear and nonlinear magneto-optical spectroscopy experiments [i.e., magneto-optical Kerr effect (MOKE) and magnetic second-harmonic generation (MSHG), respectively].

In summary, our investigation confirms the SS nature of the weakly dispersive feature detected at the M point (possibly a fingerprint of a FM surface). On the basis of both ARPES and LEED, we found that a $\sqrt{2} \times \sqrt{2}$ surface reconstruction occurs in cleaved Sr_2RuO_4, resulting in the folding of the primary electronic structure. Taking these findings into account, the FS determined by ARPES is consistent with the dHvA results and provides detailed information on the shape of α, β, and γ pockets.

We gratefully acknowledge C. Bergemann, M. Braden, T. Mizokawa, Ismail, E. W. Plummer, and A. P. Mackenzie for stimulating discussions and many useful comments. Andrea Damascelli is grateful to M. Picchietto and B. Topí for their valuable support. SSRL is operated by the DOE Office of Basic Energy Research, Division of Chemical Sciences. The office's division of Material Science provided support for this research. The Stanford work is also supported by NSF Grant No. DMR9705210 and ONR Grant No. N00014-98-1-0195.

[1] Z.-X. Shen and D. S. Dessau, Phys. Rep. **253**, 1 (1995).
[2] T. Oguchi, Phys. Rev. B **51**, 1385 (1995).
[3] D. J. Singh, Phys. Rev. B **52**, 1358 (1995).
[4] A. P. Mackenzie *et al.,* Phys. Rev. Lett. **76**, 3786 (1996).
[5] A. P. Mackenzie *et al.,* J. Phys. Soc. Jpn. **67**, 385 (1998).
[6] C. Bergemann *et al.,* Phys. Rev. Lett. **84**, 2662 (2000).
[7] D. H. Lu *et al.,* Phys. Rev. Lett. **76**, 4845 (1996).
[8] T. Yokoya *et al.,* Phys. Rev. B **54**, 13 311 (1996).
[9] A. V. Puchkov *et al.,* Phys. Rev. B **58**, R13 322 (1998).
[10] A. Liebsch and A. Lichtenstein, Phys. Rev. Lett. **84**, 1591 (2000).
[11] P. K. de Boer and R. A. de Groot, Phys. Rev. B **59**, 9894 (1999).
[12] R. Matzdorf *et al.,* Science **289**, 746 (2000).
[13] I. I. Mazin and D. J. Singh, Phys. Rev. Lett. **82**, 4324 (1999).
[14] Y. Sidis *et al.,* Phys. Rev. Lett. **83**, 3320 (1999).